

On the Continuous Formation of Field Spheroidal Galaxies in Hierarchical Models of Structure Formation

Andrew J. Benson¹, Richard S. Ellis¹ & Felipe Menanteau²

1. California Institute of Technology, MC 105-24, Pasadena, CA 91125, U.S.A. (e-mail: abenson,rse@astro.caltech.edu)

2. Carnegie Observatories, 813 Santa Barbara Street, Pasadena, CA 91101, U.S.A. (e-mail: felipe@ociw.edu)

28 October 2018

ABSTRACT

We re-examine the assembly history of field spheroidals as a potentially powerful discriminant of galaxy formation models. Whereas monolithic collapse and hierarchical, merger-driven, models suggest radically different histories for these galaxies, neither the theoretical predictions nor the observational data for field galaxies have been sufficiently reliable for precise conclusions to be drawn. A major difficulty in interpreting the observations, reviewed here, concerns the taxonomic definition of spheroidals in merger-based models. Using quantitative measures of recent star formation activity drawn from the internal properties of a sample of distant field galaxies in the Hubble Deep Fields, we undertake a new analysis to assess the continuous formation of spheroidal galaxies. Whereas abundances and redshift distributions of modelled spheroidals are fairly insensitive to their formation path, we demonstrate that the distribution and amount of blue light arising from recent mergers provides a more sensitive approach. With the limited resolved data currently available, the rate of mass assembly implied by the observed colour inhomogeneities is compared to that expected in popular Λ -dominated cold dark matter models of structure formation. These models produce as many highly inhomogeneous spheroidals as observed, but underpredict the proportion of homogeneous, passive objects. We conclude that colour inhomogeneities, particularly when combined with spectroscopic diagnostics for large, representative samples of field spheroidals, will be a more valuable test of their physical assembly history than basic source counts and redshift distributions. Securing such data should be a high priority for the Advanced Camera for Surveys on Hubble Space Telescope.

1 INTRODUCTION

The star formation and assembly history of field ‘spheroidals’ (defined here to include both ellipticals and S0s) has been discussed as one of the most powerful tests of galaxy formation capable of distinguishing between very different structure formation possibilities (Kauffmann, White & Guiderdoni 1993; Baugh, Cole & Frenk 1996b; Kauffmann & Charlot 1998a).

Traditionally spheroidals were considered to have evolved as isolated systems following a ‘monolithic’ collapse at high redshift (Eggen, Lynden-Bell & Sandage 1962). Evidence in support of this conjecture comes from many quarters, including their high central stellar density and slow rotation, consistent with non-dissipative collapse at early epochs (Efstathiou & Silk 1983), and their remarkable homogeneity at various look-back times in colour-magnitude (Sandage & Visvanathan 1978; Bower et al. 1990; Ellis et al. 1997; Stanford, Eisenhardt & Dickinson 1998) and fun-

damental plane studies (van Dokkum et al. 2001; Treu et al. 2001) of distant clusters.

This picture contrasts with that naïvely expected in models where galaxies assemble hierarchically at a rate governed by the merging of cold dark matter halos and dynamical friction timescales (Kauffmann, White & Guiderdoni 1993; Baugh, Cole & Frenk 1996b; Cole et al. 2000). Distinguishing between both hypotheses is central to verifying the cold dark matter picture but progress is hindered by the need to distinguish between star formation histories and those of mass assembly.

Most of the early work concentrated on ellipticals in rich clusters where there are significant difficulties of interpretation. The early epoch of star formation consistent with the colour-magnitude and fundamental plane studies may still be consistent with hierarchical models since clusters form from the rare, high density peaks in the primordial fluctuations within which we can expect accelerated evolution. Moreover, comparisons of galaxies in individual clusters selected at various redshifts may be fundamentally affected by

the way in which rich clusters are themselves selected. Conveniences of observation (e.g. selecting clusters of a given richness, with a relaxed distribution or of a given X-ray temperature) may bias us towards the selection of more evolved systems at a given epoch (Kauffmann 1996), thereby giving a misleading impression of a uniformly old population. Most fundamentally, if galaxies within clusters are themselves continuously evolving or arriving, it will be difficult to conduct all-inclusive inventories of a given morphological type as a function of look-back time.

For the above reasons, attention has now turned towards providing observational constraints on the evolution of *field* galaxies. The term ‘field’ here includes systems in clusters, of course, and implies an attempt to be all-inclusive in the study of the population. The simplest test for evolution in field spheroidals (and the one which has received most attention) is concerned with establishing their *number density* at high redshift, either using HST morphologies to isolate spheroidals (Zepf 1997; Schade et al. 1999; Franceschini et al. 1998; Im et al. 2001), optical-infrared colours to locate passively-evolving examples whose stars formed at high redshift (Barger et al. 1999; Daddi et al. 2000; McCarthy et al. 2001) or some combination of both (Menanteau et al. 1999).

We will show in this article that tests which rely on abundance comparisons at various redshifts or apparent magnitude limits, are currently inconclusive and, more fundamentally, are poorly-suited to discriminating between the physical details of the various assembly hypotheses. In terms of the observations, the currently available spectroscopic datasets insufficiently sample the redshift domain, $1 < z < 2$, where evolution is expected in popular low density models (Daddi et al. 2000; McCarthy et al. 2001; Firth et al. 2001). Comparisons based on counts alone are reliant on a good knowledge of the shape of the local luminosity function and its evolution. Without redshift data, there is considerable ambiguity in the implications (Glazebrook et al. 1995). In the case of samples defined morphologically from HST data, there is further confusion as to the merits of including compact objects which may possibly be unrelated star-forming galaxies whose abundance seems to increase significantly at faint magnitudes. Finally, selections based on red colours alone, even those utilising the new generation of infrared surveys, permit inclusion of unrelated dusty later-type galaxies. Colour and morphology are known to poorly correlate at low to intermediate redshifts (Schade et al. 1999) and beyond $z \simeq 1$ where dusty sources are more likely, the potential for confusion can only increase. The main drawback of abundance comparisons is that only subtle changes are expected at the depths currently being probed in low density universes, thus the significance of claims for or against the hierarchical and monolithic (or number-conserving pure luminosity evolution) models remains marginal.

Significant uncertainties are also present in the theoretical models used to interpret the observations. In semi-analytic models the build up of the stellar mass of galaxies is determined using simple arguments for cooling and star formation rates in a merging hierarchy of dark matter halos. Even granting this very simple prescription, there is a

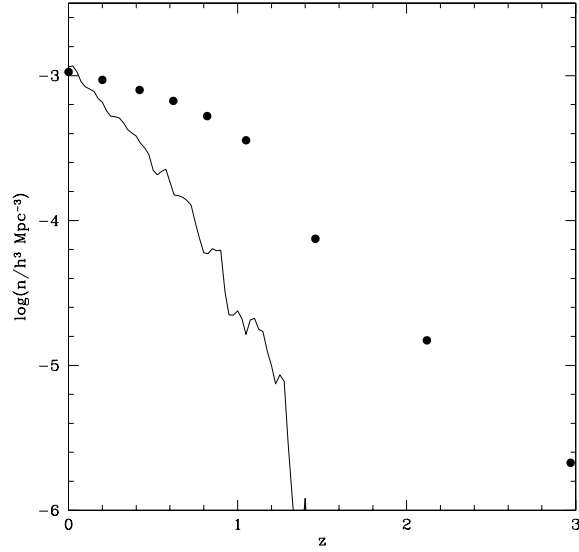


Figure 1. Theoretical uncertainties in the evolutionary history of massive spheroidals: the solid line and circles show the comoving density of all galaxies with stellar mass greater than $10^{11} M_\odot$ as a function of redshift in the Λ CDM models of Cole et al. (2000) and Kauffmann et al. (1999) respectively.

surprising uncertainty concerning the expected evolution in the number density of massive systems. For example, we can consider the comoving abundance of objects selected by stellar mass as a function of redshift. In Fig. 1 the solid line and circles show the comoving abundance of galaxies with stellar masses greater than $10^{11} M_\odot$ in a Λ CDM cosmology as predicted by Cole et al. (2000) and Kauffmann et al. (1999) respectively. (Note that while the basic cosmological parameters, Ω_0 and Λ_0 were the same for these two calculations others, including Ω_b , were different. The Cole et al. (2000) results are taken from the models used in this paper, while those of Kauffmann et al. (1999) were computed from their publicly available galaxy catalogues.) Although the two models are in reasonable agreement at $z = 0$ only rather modest evolution (about a factor three decline) is predicted to $z \simeq 1$ by Kauffmann et al. (1999), whereas much stronger evolution is expected according to the model of Cole et al. (2000).

This discrepancy in the rate of evolution predicted by two similar models is very worrying, although it should be remembered that the galaxy stellar mass function is steep in this region. Hence even minor differences in the rate at which galaxy masses evolve in the two models could lead to large differences in abundance. For example, the factor of 10 difference at $z = 1$ might be resolved by considering galaxies only a factor of 2 less massive in the Cole et al. model. Nevertheless, it is evidently crucial to understand these differences before strong tests of the hierarchical hypothesis can be made.

A recent analysis of spheroidals in both Hubble Deep Fields (HDF) by Menanteau, Abraham & Ellis (2001) offers an interesting opportunity to bypass many of the difficulties

discussed above. Resolved V – I colour data for the HDF spheroidals reveals the presence of blue cores in a significant subset and preliminary spectroscopy (c.f. Ellis 2000) confirms that recent star formation is the likely cause. Together with a careful appraisal of the way in which spheroidal galaxies are defined in semi-analytic models, further analysis of this dataset forms the basis of the present paper. Instead of making absolute count comparisons, we use the distribution of colour inhomogeneities to determine the fraction of spheroids still assembling. We compare this with hierarchical predictions taking into account the selection technique and uncertainties arising from the taxonomical definition of a recognisable spheroidal galaxy. This type of comparison, in which the information of interest is encoded in a complex way in the data and important selection criteria exist, is one of the key areas where semi-analytic models excel. Most significantly, we demonstrate that such an analysis, based on post-merger relaxed systems with residual star formation, is a more direct test of the pertinent assembly details than traditional techniques based on counts or luminosities alone.

A plan of the paper follows. In §2 we discuss the various ways in which spheroidals can be defined in hierarchical models, introducing a definition that incorporates a timescale for relaxation to a spheroidal form. We test predictions utilising these definitions against published morphological number counts (Glazebrook et al. 1995; Driver et al. 1995a, 1995b; Franceschini et al. 1998) and redshift distributions (Brinchmann 1999; Menanteau et al. 1999). In §3 we revisit the observational analysis of Menanteau et al., and compare theory with observation in the light of both observational and theoretical uncertainties. We summarise our conclusions in §4.

2 SPHEROIDAL GALAXIES IN HIERARCHICAL MODELS

2.1 Semi-Analytic Modelling and Morphological Evolution

First we discuss the basic processes which govern the mass assembly and star formation histories of spheroidals in hierarchical models. Specifically, we will utilise the galaxy formation model described by Cole et al. (2000) to which the reader is referred for a full description. Here we summarise briefly the salient features. A small number of model parameters are crucial in determining the properties of the spheroids in which we are interested as described below. Cole et al. describe how these model parameters may be constrained by a set of $z = 0$ observational data. We retain the same parameter values which Cole et al. found produced the best agreement with the local data. As such, the model results presented in this work are true predictions. In §3 we will consider the effects of changing some of these parameters (and also in altering the basic mechanisms by which spheroidal galaxies are made) as a way to understand the model results and to test their robustness and also to ascertain the prospects of our approach for directly constraining the formation history of spheroidals. It must be kept in mind however, that once a parameter value is changed the model

is unlikely to remain a good fit to the local data and so any such results cannot be considered to be predictions of a realistic hierarchical model.

In this model, galaxies form continuously from cooling gas inside a dark matter halo. Gas settles into a disk configuration within which stars form quiescently. Spheroidal galaxies are produced by a major merger of two pre-existing galaxies of comparable mass (note that the pre-existing galaxies may be disks, spheroids or a mixture of both, and that disks may contain both stars and gas), which occurs due to dynamical friction (the timescale of which is determined by a parameter of the model, f_{df} , which is set to 1 unless otherwise stated) dissipating energy from the galaxies' orbits. Such a merger disrupts the galaxies leaving a spheroidal remnant, and also triggers any cold gas present to undergo a burst of star formation with an exponentially decreasing star formation rate. The spheroidal so formed may accrete gas through cooling at a later time and thereby grow a new disk. Model galaxies can thus migrate either way along the Hubble sequence, and may change their morphologies several times during their lifetimes.

Only a major merger (defined as one in which $M_1/M_2 \geq f_{\text{ellip}}$, where M_1 and M_2 are the masses of the merging components with $M_1 \leq M_2$ and f_{ellip} is a parameter of the model) triggers a burst of star formation. The timescale of the burst is $\tau_{\text{burst}} = \epsilon_{*,\text{burst}}^{-1} \tau_{\text{dyn}}$, where τ_{dyn} is the dynamical time of the newly formed spheroid and $\epsilon_{*,\text{burst}}$ is a free parameter.

Cole et al. (2000) chose $f_{\text{ellip}} = 0.3$, as suggested by numerical simulations (Walker, Mihos & Hernquist 1996; Barnes 1998) which show that the merging galaxy mass ratio must be in the range 0.3 to 1.0 to destroy the progenitor components and produce a spheroidal remnant. The value of $\epsilon_{*,\text{burst}}$ is best constrained by the luminosities of bursting galaxies since these are directly related to the star formation rate in the burst. To accurately predict the luminosities of starbursts a detailed treatment of the absorption and reprocessing of light by dust is needed. Such an analysis has been carried out by Granato et al. (2000), who found that $\epsilon_{*,\text{burst}} = 0.5$ provided the best fit to the $z = 0$, $60\mu\text{m}$ galaxy luminosity function (in which we see light absorbed and re-emitted by dust in starbursts) so we will adopt this value as default in this work.

Spheroidals may also form via the gradual accretion of smaller galaxies (minor mergers). In the case of a minor merger ($M_1/M_2 < f_{\text{ellip}}$) we assume no burst of star formation is involved. Stars from the smaller galaxy are added to the bulge of the larger galaxy, which may then become dominant, while any residual gas is added to its disk.

2.2 Model Comparisons based on Number Counts and Redshift Distributions

In this section we are concerned with exploring those parameters central to the taxonomical definition of a morphological spheroidal. The majority of previous studies using semi-analytic models to study the properties of galaxies selected by their morphological type (Kauffmann 1996; Baugh, Cole & Frenk 1996a,b; Kauffmann & Charlot 1998a) have used

the bulge-to-total ratio, B/T , usually (as here) measured in terms of luminosity. (Specifically, in this work we use the dust-extinguished I_{814} -band luminosity to define the bulge-to-total ratio, $B/T_{I_{814}}$.) Baugh, Cole & Frenk (1996a) also considered the time since the most recent major merger for each galaxy to be a defining property, placing galaxies whose last major merger occurred less than 1 Gyr earlier into the Irr/Pec category. Accordingly, spheroidals in the Baugh, Cole & Frenk (1996a) scheme jointly satisfy $B/T > 0.4$ and have experienced no major merger in the last 1 Gyr.

The key issue, central to a successful interpretation of the resolved colour data, is that spheroidals can appear to be dynamically relaxed while showing evidence of recent star formation (e.g. in their internal colours). Instead of adopting a fixed relaxation period to define a semi-analytical spheroidal, we include a criterion based on the dynamical timescale of the remnant. After a major merger, the remnant begins to relax from the inside out in a time comparable to the local dynamical time (Barnes & Hernquist 1992). For each remnant we calculate the dynamical time at the half-mass radius. Any object which experienced a major merger less than N_{relax} dynamical times ago is considered to be an Irr/Pec galaxy, irrespective of its B/T . N_{relax} is a parameter of the model which we expect to be of order unity. For the sample of galaxies considered in this work, spheroidal dynamical times are typically a few times 10^7 years, i.e. much shorter than 1 Gyr. Crucially, for small values of N_{relax} , a merger remnant can be classed as relaxed well before the distinctive blue colour of recent star formation activity has declined.

We summarise our scheme for defining a sample of morphological spheroidals in Table 1. Since in this work we are primarily interested in the E/S0 class only the parameters B/T_S and N_{relax} need to be constrained. As such, we will not attempt to constrain the values of the other parameters in Table 1. Although Cole et al. (2000) briefly considered the morphological mix of bright galaxies, they did not explore in detail the sensitivity of their parameter choices to data on morphologically selected faint galaxies. As noted by Baugh, Cole & Frenk (1996b) we have some guidance as to the value of B/T_S from comparisons of galaxy T-types with their bulge-to-total ratio obtained from bulge/disk decomposition studies. Such comparisons suggest $B/T_S \approx 0.4$, but with significant uncertainty. Keeping this figure in mind, we now explore what constraints can be set on B/T_S and N_{relax} from the available observational data, specifically morphologically selected number counts and redshift distributions.

Number counts are only weakly dependent on the assumed model parameters. Figure 2 shows the E/S0 and total number counts in the I_{814} band¹; clearly the baseline model (solid lines) matches these data very well. The key question is the extent to which the morphologically-classified counts depend on our parameters B/T_S and N_{relax} . Both the S and Irr/Pec number counts (not shown) are relatively insensitive to the value of N_{relax} and thus constrain the parameter B/T_S to be $\lesssim 0.44$ (in good agreement with the figure expected from a comparison to T-types). A value as low

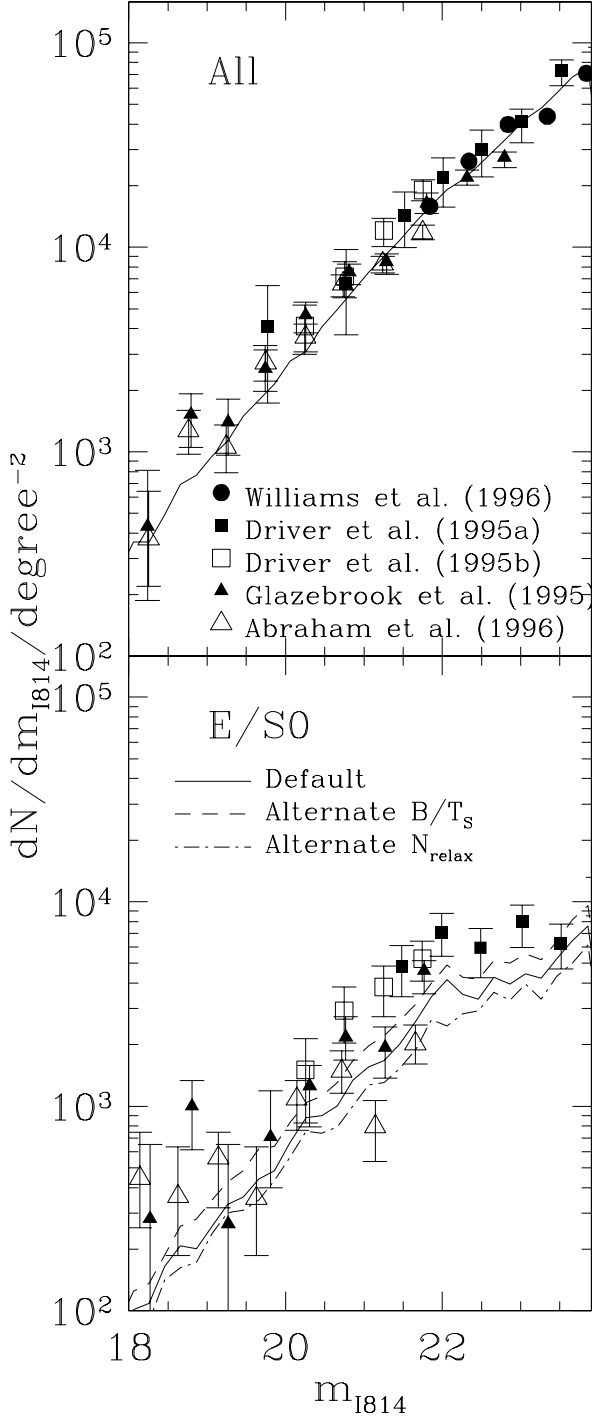


Figure 2. Differential number counts in the I_{814} pass-band as a function of morphological type. Panels show the counts for all galaxies (top) and E/S0 galaxies (bottom). Points show a compilation of observational determinations (as indicated in the upper panel) while lines show the model results (solid line — default parameters; dashed line — alternative B/T_S ; dot-dashed line — alternative N_{relax}).

¹ We use Vega-based magnitudes throughout this paper.

Table 1. Morphological classification scheme. Galaxies are classified on the basis of their bulge-to-total ratio in dust-extinguished I-band light, B/T_{I814} (column 1), and the ratio of the time since the last burst of star formation to the dynamical time of the spheroid, $t_{\text{burst}}/t_{\text{dyn}}$ (column 2). The morphological class assigned to each region of this two-parameter space is given in column 3.

B/T_{I814}	$t_{\text{burst}}/t_{\text{dyn}}$	Morphological class
$0 \leq B/T \leq B/T_{\text{Irr}}$	$> N_{\text{relax}}$	Irr
$B/T_{\text{Irr}} < B/T \leq B/T_S$	$> N_{\text{relax}}$	S
$B/T_S < B/T \leq 1$	$> N_{\text{relax}}$	E/S0
$0 \leq B/T \leq 1$	$\leq N_{\text{relax}}$	Pec

Table 2. Parameters of the relevant morphological classification schemes (but which do not affect the merging and formation histories of model galaxies).

Parameter	Parameter set		
	Default	Alt. B/T_S	Alt. N_{relax}
B/T_S	0.44	0.30	0.44
N_{relax}	3	3	30

as $B/T_S = 0.30$ remains consistent with the counts, while lower values begin to underpredict the number of spirals. The predicted E/S0 counts are quite insensitive to N_{relax} for $N_{\text{relax}} \lesssim 10$. The dot-dashed line in Fig. 2 shows the results for $N_{\text{relax}} = 30$, which begins to deplete the number of E/S0 galaxies below that observed. While the counts suggest a reasonably low value of N_{relax} , they do not provide a strong constraint. This insensitivity might be perceived as an advantage; a detail in the assembly history is irrelevant in interpreting an observable. However, as the relaxation timescale is central to the rate at which systems become recognisable spheroidals, this would be false security, particularly in diagnosing systems at high redshift.

In the light of the above constraints, in the remainder of this paper we will consider three sets of values for the parameters B/T_S and N_{relax} as listed in Table 2. Note that these parameters determine only the morphological classification scheme and, as such, we would ideally constrain them accurately from morphologically selected number counts, redshift data etc. Later, we will consider altering other parameters of the model which directly alter the formation and merging histories of model galaxies. It is these formation and merging rates which we aim to constrain through the methods described in this paper.

In the upper two panels of Fig. 3 we compare the redshift distribution of model galaxies in magnitude limited samples with the recent HST-based redshifts surveys as summarised by Brinchmann (1999). These encompass the initial survey of Schade et al. (1999) enlarged to include a total of 54 spheroidals spectroscopically-complete to $I_{814} = 22$. Additional data to a somewhat brighter magnitude limit is in principle available from the survey of Im et al. (1999) and Im et al. (2001). However, we chose not to include this sample as the spheroidals were defined according to symmetry and colour, i.e. differently than in Figure 2. Im et al. (2001) discuss the uncertainties of their definition which

affect the absolute abundances at the $\simeq \pm 25\%$ level. As expected, the proportion of high redshift spheroidals is sensitive to N_{relax} , with larger values producing fewer examples (since more galaxies are placed into the Irr/Pec class). Unfortunately, although the range of redshifts spanned by the model galaxies is comparable to that seen in the data, the detailed correspondence between theory and observations is not particularly good for the total sample (upper panel), a point discussed by Baugh, Cole & Frenk (1996a).

The lower panel of Fig. 3 shows the deeper ($I_{814} < 24$) E/S0 sample of Menanteau et al. (1999), which is employed extensively in this paper. Barring one discrepant point, the model is in very good agreement with this redshift distribution. The differences between the model predictions for the three parameter sets illustrate again how well these parameters could be constrained by larger datasets.

While our baseline semi-analytical model, in which spheroidals are formed by the mergers of two pre-existing galaxies, produces some of the observed trends in this population, at a quantitative level it disagrees with the present redshift data. More relevant at this stage, however, is the poor sensitivity of such observables to key physical features of the hierarchical model. Even with exquisite data at these magnitude limits, we can expect it will be hard to conclusively determine whether the hierarchical model is correct given the freedoms in the morphological definitions introduced in Table 1. Therefore, we propose to use these observational data to constrain the morphological classification parameters of Table 1 and then use other data, such as that described in this paper, to constrain the formation and merger rates of spheroidals.

2.3 Quantifying Recent Activity Using Colour-Based Properties

In the present section we demonstrate that the colour inhomogeneities discovered for HDF spheroidals (Menanteau, Abraham & Ellis 2001) offer a much more direct probe of the hierarchical hypothesis than the number count and redshift distributions discussed in §2.2. Not only do the *internal* colour variations seen in the HDF offer an important way to separate models based on isolated passive evolution following monolithic collapse from those invoking continuous hierarchical assembly, but they also provide the first opportunity for a quantitative measure of the assembly rate in the latter case. Importantly, Menanteau, Abraham & Ellis (2001) find that around one third of spheroidals in their sample show marked inhomogeneities in their internal colours, and that in the majority of these cases the inhomogeneity is characterised by a blue core in the galaxy colour profile. The observations therefore require that blue light be more centrally concentrated than red light. Here we will assume that these blue cores arise due to recent bursts of star formation.

For present purposes, where we are concerned only with V and I photometry, the major merger event which forms each elliptical in the model can be characterised by two physical quantities: (i) the fraction of stars formed in the associated burst relative to the final stellar mass of the spheroidal

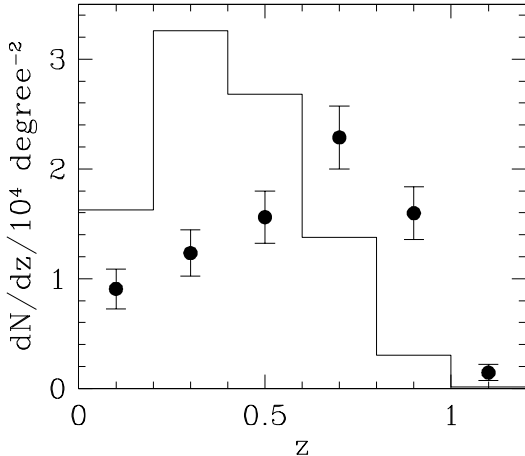
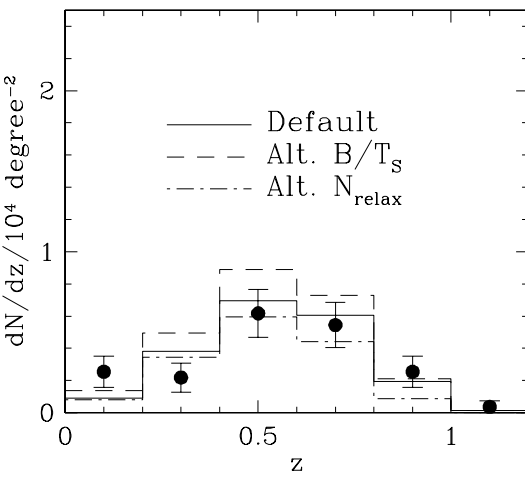
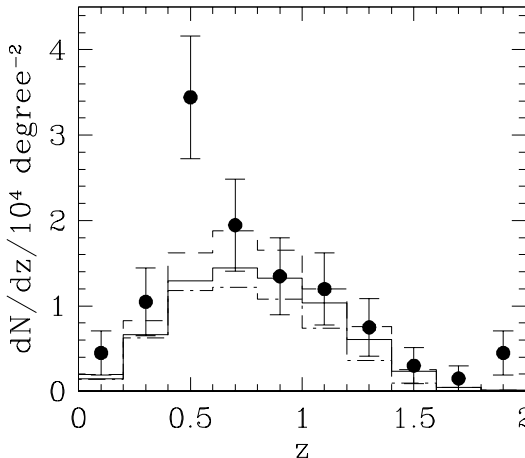
Brinchmann et al. (2000) : All : $I_{814} < 22$ Brinchmann et al. (2000) : E/S0 : $I_{814} < 22$ Menanteau et al. (2001) : E/S0 : $I_{814} < 24$ **Figure 3.**

Figure 3. (cont.) The three panels show faint galaxy redshift distributions, with observational data indicated by filled circles and model predictions shown as histograms. In the upper panel we show the redshift distribution of galaxies of all morphological types brighter than $I_{814} = 22$ from Brinchmann (1999), while the middle panel shows the redshift distribution of spheroidal galaxies from the same sample. The lower panel shows the redshift distribution of $I_{814} < 24$ spheroidals from Menanteau et al. (1999). In the lower two panels, model results are shown for standard (solid histogram), alternative B/T_S (dashed histogram) and alternative N_{relax} (dot-dashed histogram) parameters.

remnant, f_{burst} , and (ii) the time since the merger, t_{burst}^2 . The first determines how the colour of the remnant evolves with time, and which can in principle be constrained by the resolved HDF data, and the second determines at what point in that evolution the galaxy is observed. Ideally we would like to measure these two parameters directly from the observational data as this would allow us to reconstruct the rate of spheroid formation as a function of redshift. However, with the present photometric data and relatively small sample size such an approach is not warranted (spectroscopic measurements will provide far better constraints on these parameters). Instead we focus on the much simpler objective of assessing the compatibility of hierarchical formation with the present data. However, we will give predictions for the variation of these key parameters with redshift which may then be tested by forthcoming observations.

In Fig. 4 we show how the two physical quantities vary with redshift for a magnitude-limited sample of model galaxies in a Λ CDM cosmology. In this and subsequent figures, we will consider spheroidal galaxies brighter than $I_{814} = 24$ in order to match the HDF sample used by Menanteau, Abraham & Ellis (2001). Unless otherwise stated all model results refer to our default parameters (refer to Table 2).

There is little variation in f_{burst} with redshift, but a significant dispersion at fixed z . The median burst typically involves 10-20% of the total spheroidal mass. The lack of any trend with redshift is the result of two counteracting effects. Firstly, f_{burst} shows a strong correlation with the mass of the spheroidal galaxy, such that lower mass galaxies tend to have higher values of f_{burst} . This trend arises because more massive ellipticals tend to form from more massive disk progenitors Kauffmann & Charlot (1998a) and, in the model of Cole et al. (2000), more massive disks tend to have smaller gas fractions (at least if we consider only central galaxies, which are always involved in the formation of an elliptical), a consequence of the variation of star formation rate with disk mass.

The apparent magnitude limit of the sample prevents us from seeing the least massive (highest f_{burst}) galaxies at high redshifts. However, at high redshift there are also fewer of the most massive (lowest f_{burst}) galaxies (since these have not had time to form).

² The metallicities of pre-existing and newly-formed stars will also have some effect on the colours, an effect correctly accounted for in the model, but is of secondary importance to the present discussion.

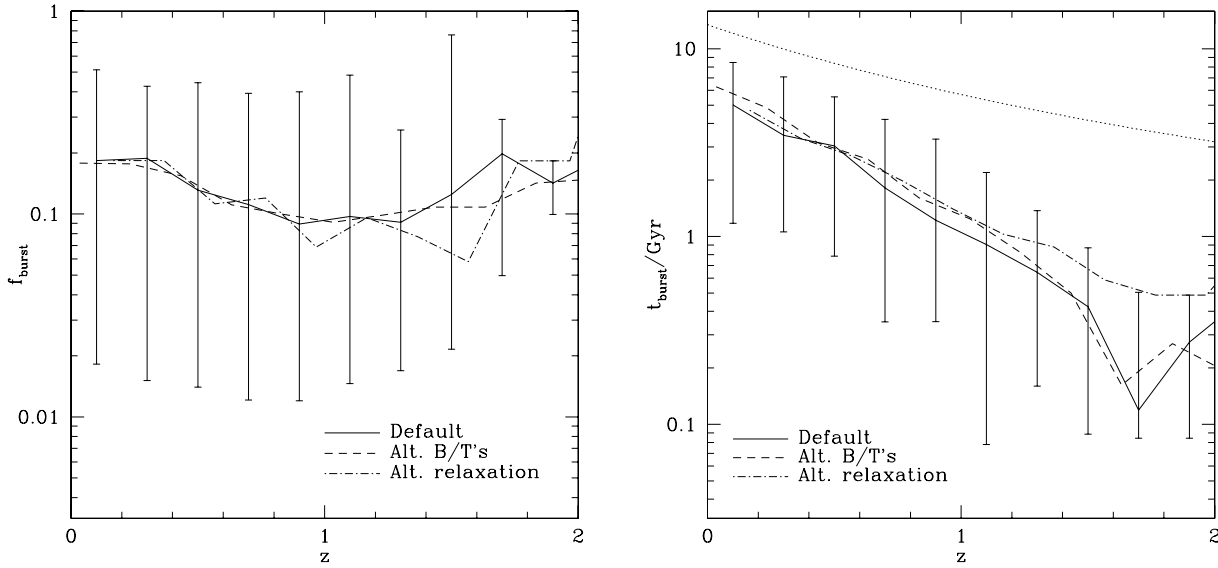


Figure 4. The variation with redshift of the two parameters defining a merger event, f_{burst} and t_{burst} (left and right-hand panels respectively). Lines show the median of the model relation with error bars indicating the 10% and 90% intervals. Solid lines show results for our default parameters, dashed and dot-dashed for the alternative B/T_S and N_{relax} respectively. For clarity, error bars are shown only on the solid lines. The 10% and 90% intervals for the other models are comparable to the default model with the exception that the 10% intervals of t_{burst} for the alternative N_{relax} model occur at significantly larger t_{burst} .

There is a strong trend of t_{burst} with redshift however. This quantity is bounded by the age of the universe at given z (since no galaxy can have experienced a burst which began earlier than $t=0$). The dotted line in Fig. 4 shows the age of the universe as a function of redshift. The evolution in the median value of t_{burst} is much more rapid than this. This is a consequence of higher rates of merging at high redshift combined with the fact that, at high redshift, a galaxy is seen only if it is intrinsically luminous and so we preferentially select galaxies which have recently experienced a burst of star formation, these being more luminous than quiescent examples (particularly in view of the k-correction at $z \approx 1.5$).

In conclusion the model predicts that for the magnitude limited sample considered here, a strong correlation between t_{burst} and redshift should exist, such that higher redshift spheroidals have typically experienced a burst more recently.

We now describe how we measure the degree of recent activity in a spheroidal galaxy from the available photometric data (both real observational data and mock images of model galaxies). Menanteau, Abraham & Ellis (2001) proposed a statistic $\delta(V-I)$ which measures the degree of inhomogeneity in the internal colours defined as:

$$\delta(V-I) = 2N \frac{\sum (x_i - \bar{x}_i)^2 S(x_i) \text{SNR}(x_i)}{\sum S(x_i) \text{SNR}(x_i)}, \quad (1)$$

where x_i is the colour of the i^{th} pixel, $\text{SNR}(x_i)$ is the signal to noise ratio, $S(x_i)$ is a step function which includes only those pixels with $\text{SNR}(x_i) > 1.3$ in the sum and N is an arbitrary constant which was taken to be $N = 3$. The sum is taken over all pixels brighter than $V_{606} = 25.5 \text{mag}$

arcsec^{-2} . The value of $\delta(V-I)$ obtained for any single galaxy will depend on the point spread function (PSF) of the observing instrument, since substantial smoothing will tend to homogenise the internal colours. Although wavelength dependent PSFs, such as occur in the WFPC2, can create artificial colour inhomogeneities. Menanteau, Abraham & Ellis (2001) found this to be a negligible source of inhomogeneity for the HDF spheroidals except for a few galaxies with highly concentrated surface brightness profiles.

As an alternative diagnostic we consider the difference in integrated colour compared to that expected at the galaxy redshift for an old, passively evolving population, $(V-I)_{\text{passive}}(z)$. The latter case is defined here as a system which formed at $z_F = 3$ with an exponentially decaying star formation rate with e-folding time of 1 Gyr and with Solar metallicity. In Fig. 5 we show the integrated $V-I$ colours of observed and model spheroidal galaxies as a function of redshift and compare these to $(V-I)_{\text{passive}}(z)$. We plot data from the HDF sample of Menanteau, Abraham & Ellis (2001) and also from the brighter ($I_{\text{AB}} < 22$) sample of Schade et al. (1999) to demonstrate that both datasets display similar trends. Note that while both model and data broadly trace out the shape of the passive curve, both reveal many galaxies that are significantly bluer. This is particularly noticeable for the model at $z \gtrsim 1$ where the median colour is ~ 0.3 magnitudes bluer than the passive prediction.

Interestingly, the HDF data also contains a few very red objects (i.e. redder than the passively evolving track shown in Fig. 5, and in fact redder than passively evolving tracks for galaxies formed even at higher z_F). The most anomalous

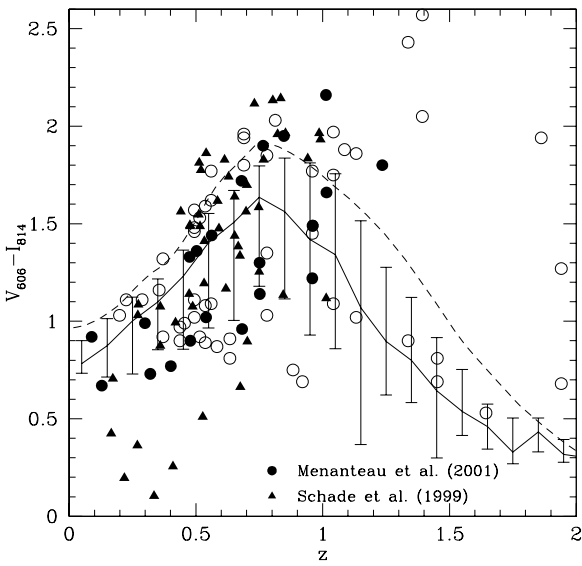


Figure 5. Integrated V–I colour as a function of redshift. Circles show data from the HDF North and South with solid points indicating spectroscopic redshifts and open points photometric redshifts. Triangles show brighter data from the survey of Schade et al. (1999) (with morphologies classified visually). The median of the model distribution is shown by the solid line, with error bars indicating 10% and 90% intervals of the distribution. The dashed line indicates the colour of a galaxy formed at $z = 3$ with an exponentially decaying star formation rate with e-folding time of 1 Gyr and with Solar metallicity.

lous sources are ones with photometric redshifts above unity. The red colours could arise as a consequence of an overestimated photometric redshift although two of these galaxies would be extremely red whatever redshift they were placed at. Certainly, Fig. 5 suggests that our present model does not produce spheroidal galaxies as red as those observed in the HDF.

We define the colour excess:

$$(V - I)_{\text{excess}} = (V - I) - (V - I)_{\text{passive}}(z). \quad (2)$$

While this simple measure has the desirable property of being largely independent of the PSF it makes no use of the resolved internal structure, and furthermore is sensitive to errors in the redshift of the galaxy (which is particularly important for the galaxies with only photometric redshifts). Nevertheless, it is interesting to compare this measure with the $\delta(V - I)$ index.

To determine the sensitivity of both statistics for the model galaxies we construct a mock image of each galaxy (including noise which makes a small contribution to $\delta(V - I)$), smoothed with a Gaussian PSF of FWHM 0.126 and 0.143 arcseconds in the V and I-bands respectively to mimic the PSF of the WFPC-2 (Casertano et al. 2000). Both statistics described above are then measured as for a real galaxy. For the purposes of constructing mock images each galaxy is assumed to consist of three components, a disk, a spheroidal remnant and a recent burst. Although a galaxy

may have experienced more than one burst in its history we treat only the stars formed in the most recent burst as a separate component, with stars which were formed in earlier bursts assumed to be uniformly mixed in the spheroidal component. Our results are insensitive to this assumption, since placing the light from stars formed in all the bursts in a separate component does not make any significant difference to the statistics we consider.) Disks are modelled with an exponential surface brightness profile and random inclination. Hernquist (1992) has shown that mergers between purely stellar systems, specifically bulge-less galaxies, result in a remnant which has a surface brightness profile close to an $r^{1/4}$ -law, but with a core of constant surface brightness. A simple parameterisation which displays qualitatively similar behaviour is

$$\Sigma(r) = \Sigma_0 \exp \left(-7.67 \left[([r/r_e]^2 + c^2)^{1/8} - 1 \right] \right), \quad (3)$$

where r is the radius, r_e the effective radius and c is a core radius in units of r_e . We will refer to this form as the ‘‘Hernquist profile’’ hereafter. This expression is not proposed as an accurate fit to the Hernquist (1992) results, but has the desirable properties of being analytically integrable and able to produce remnants with any desired core size. We distribute the mass of the pre-existing stars with this surface density profile. Gas in mergers is generally driven to the centre of the remnant where it presumably undergoes a burst of star formation (Barnes & Hernquist 1996). The stars formed in the recent burst are therefore distributed in such a way that the total surface mass density (i.e. the sum of burst and pre-existing components) follows an $r^{1/4}$ -law (i.e. as eqn. 3 with $c = 0$). The total mass in the Hernquist profile is given by $M(c) = \int_0^\infty 2\pi r \Sigma(r) dr$. Requiring that $M(c)/M(0) = M_{\text{burst}}/(M_{\text{burst}} + M_{\text{pre}})$, where M_{burst} is the mass of the stars formed in the burst and M_{pre} is the pre-existing stellar mass, allows us to solve for c . The value of r_e is determined from the half-mass radius of the remnant as calculated by the galaxy formation model (Cole et al. 2000). The light of each component is then distributed as the mass assuming a constant mass-to-light ratio. With this construction the spheroid would eventually come to resemble an $r^{1/4}$ -law at late times when the stars of both components were old (ignoring any differences in metallicity between the two populations).

In cases where the recent burst accounts for a large fraction of the total mass of the spheroid the core radius, c , can become very large. No simulations of mergers between such gas-rich disks have been carried out (but see Somerville, Primack & Faber 2001), so the above form for the pre-existing and burst star populations may not be relevant in such cases. We therefore consider an alternative case in which both pre-existing and burst stars are distributed as $r^{1/4}$ -law profiles, but with the burst stars having a much smaller effective radius (one tenth of the spheroid radius).

3 ANALYSING RECENT ACTIVITY IN HDF ELLIPTICALS

We now compare the distributions of model and observed HDF spheroidal galaxies using the two statistics described in §2.3.

The lower left-hand panel of Fig. 6 shows differential distributions of each statistic. For $(V - I)_{\text{excess}}$ the model produces a comparable distribution to the data for blue objects ($(V - I)_{\text{excess}} \lesssim 0$), but cannot account for the red objects ($(V - I)_{\text{excess}} \gtrsim 0$) as was expected on the basis of Fig. 5. This quantity is independent of the surface brightness profiles we ascribe to model galaxies, but does depend on the values of the parameters B/T_S and N_{relax} . In the lower right-hand panel of Fig. 6 we demonstrate the effects of using the alternative parameter values given in Table 2. Using $B/T_S = 0.30$ instead of 0.44 produces substantially more galaxies just bluewards of $(V - I)_{\text{excess}} = 0$ (this alternative morphological definition tends to include several galaxies which experienced their last burst much longer than 1Gyr ago and whose only star formation is occurring in their disks), without affecting the rest of the distribution. Increasing N_{relax} from 3 to 30 significantly reduces the number of very blue model galaxies. With the larger value of N_{relax} these extremely blue galaxies, which have typically experienced a major merger in the very recent past, are rejected from the E/S0 class. With the present data we can infer $N_{\text{relax}} \lesssim 10$. Note that neither of these parameter alterations helps reconcile the observed and predicted distributions of red galaxies.

For $\delta(V - I)$ we show two model lines in the upper left-hand panel, the solid one using the Hernquist profile and the dashed one using an $r^{1/4}$ -law for both burst and pre-existing stellar components. The choice of profile does not drastically alter the width or shape of the distribution. Using $r^{1/4}$ -law profiles produces somewhat more galaxies at low values of $\delta(V - I)$ and does not produce the tail to high values which occurs with the Hernquist profile. We remind the reader that while the Hernquist profile has some theoretical justification, the $r^{1/4}$ -law profile has none. The purpose of considering this profile is to demonstrate that the model predictions are not overly sensitive to this choice.

In the upper left-hand panel we again see that the model distribution is in reasonable agreement with the data for high values of $\delta(V - I)$, but appears to predict too few galaxies with low $\delta(V - I)$. In the upper right-hand panel we consider the effects of changing model parameters on the predictions for $\delta(V - I)$. Changing B/T_S from 0.44 to 0.30 produces more model galaxies at low $\delta(V - I)$, thereby improving the agreement between model and data (although some differences remain), while increasing N_{relax} to 30 depletes the number of galaxies at all $\delta(V - I)$, but particularly so at high $\delta(V - I)$ since these galaxies are those which have experienced a major merger in the very recent past. However, even with this large value of N_{relax} (which is marginally ruled out by the morphologically selected counts of Fig. 2) the model still provides a reasonable match to the high $\delta(V - I)$ data.

Finally, in Fig. 7, we compare model and data as a function of redshift. For the model the median relation is shown

by the line, with error bars showing the 10% and 90% intervals at each redshift. Error bars are typically shown on only one line per panel to aid clarity but are of comparable size for the other lines. Data are shown by circles; filled and open to indicate spectroscopic and photometric redshifts respectively. As shown in the upper panels, both model and data show an increasing median $\delta(V - I)$ with redshift out to $z \approx 1$. The top left-hand panel clearly demonstrates that the model predictions for $\delta(V - I)$ at high redshifts depend crucially on the surface brightness profile adopted for the post-merger spheroidal, with the Hernquist profile producing many more high $\delta(V - I)$ galaxies at high redshift than the $r^{1/4}$ profile (for which the distribution of $\delta(V - I)$ is in rather good agreement with the data at all redshifts). The exact choice of model parameters has little effect on the prediction (although increasing N_{relax} to 30 does reduce the 90% intervals).

In $(V - I)_{\text{excess}}$ (lower panels) the model spans a similar range to the data as a function of redshift, the rapid increase in blue excess objects between $z = 0$ and $z = 0.5$ is apparent in both model and data for example. Interestingly, the data appears almost bimodal at these redshifts, with one group of galaxies lying along $(V - I)_{\text{excess}} \approx 0$ (and so are presumably old, passive spheroidals) and another group lying along a locus of $(V - I)_{\text{excess}}$ which decreases with redshift. Dots show a sample of model galaxies for comparison. Although a clear branch of model points can be seen running along $(V - I)_{\text{excess}} \approx 0$, no well-defined branch is seen in the vicinity of the second group of data points, although the model points certainly span the range of blue $(V - I)_{\text{excess}}$ values seen in the data. Given the small number of data points (and the fact that most of those in the second branch have only photometric redshifts) no strong conclusions can be drawn as yet. Of course, the model does not contain the very red galaxies seen in the data, as expected from Fig. 5.

Since we can easily switch off the effects of the PSF on model galaxies we have checked that the wavelength dependence of the PSF does not significantly affect the distribution of $\delta(V - I)$ for model galaxies. Without the PSF the distribution of $\delta(V - I)$ for model galaxies is significantly higher in the lowest bin of $\delta(V - I)$ shown in Fig. 6 (the wavelength dependence of the PSF increases $\delta(V - I)$ for a few of these galaxies, mostly at low redshifts, giving them $\delta(V - I) \approx 0.1$) and the tail extends to slightly higher $\delta(V - I)$ (here it is the homogenising effects of the PSF which are important, particularly for high redshift galaxies).

We have also checked the effect of the disk component of the model spheroidal galaxies. Recall that our E/S0 class contains galaxies with at least 44% of their light in a spheroidal component, allowing up to 56% to be in a disk (although many have much less than this of course). The disk light can contribute to $\delta(V - I)$ and $(V - I)_{\text{excess}}$ since it may be of a different colour to the spheroidal light and is also distributed differently. The broad features (e.g. width) of the $\delta(V - I)$ and $(V - I)_{\text{excess}}$ distributions remain the same whether we include the disk components of E/S0 galaxies or not.

Without the disk component we find that the tail of the $\delta(V - I)$ distribution extends to slightly higher values

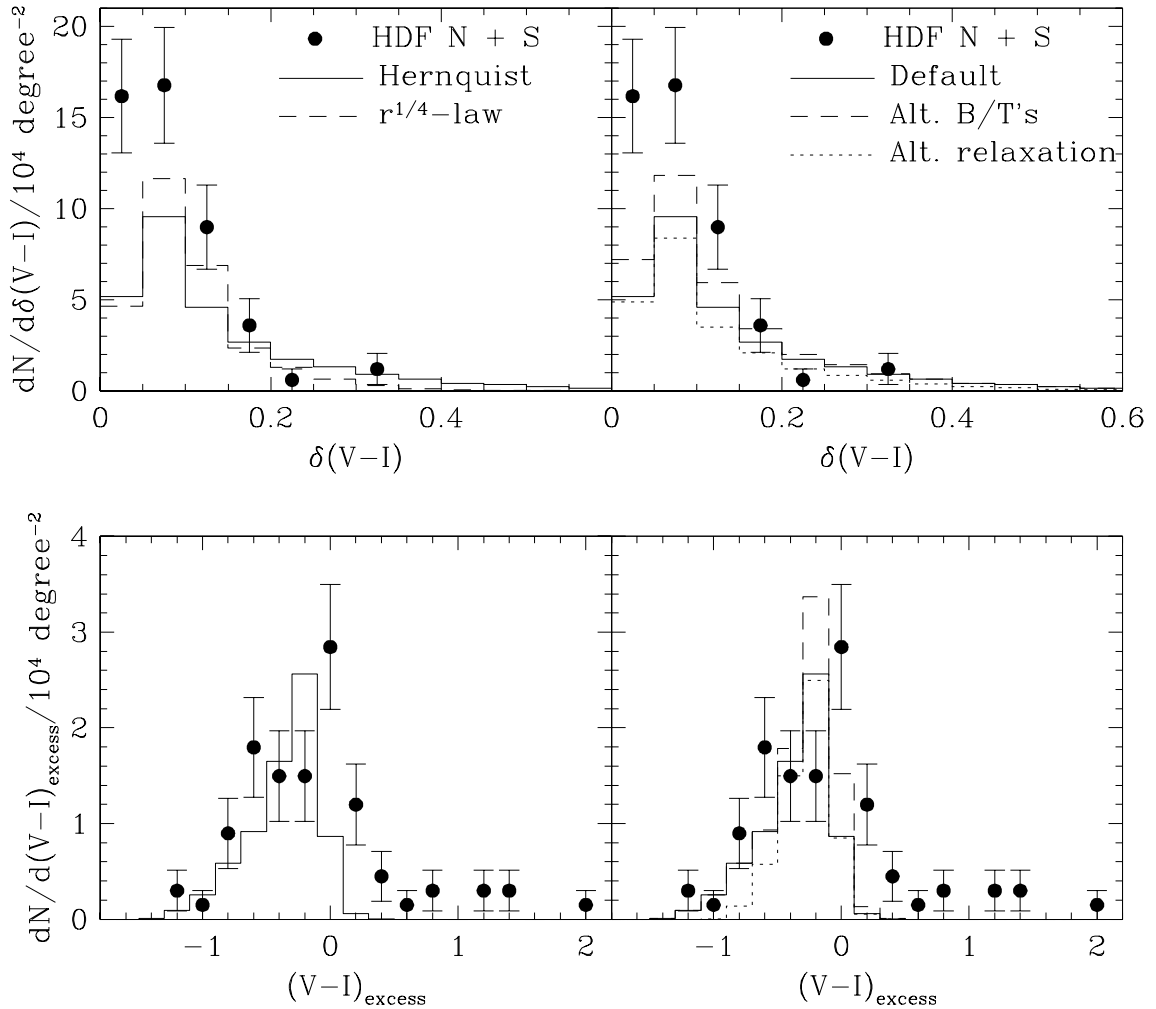


Figure 6. Differential distributions of both statistics discussed in §2.3 for E/S0 galaxies brighter than $I_{814} = 24$. Circles show observational data from the combined HDF North & South. Histograms show model results. In the left-hand column solid histograms are for the Hernquist profile, while dashed histograms use an $r^{1/4}$ -law profile. In the right-hand column solid lines are for the default parameters, dashed for for alternative B/Ts and dotted for alternative N_{relax} .

(in galaxies with a recent burst adding a disk component can actually reduce $\delta(V - I)$ since the disk may be of similar colour to the burst component), but the effect is small relative to the current theoretical and observational uncertainties. In $(V - I)_{\text{excess}}$ leaving out the disk components reduces the number of galaxies at $(V - I)_{\text{excess}} \approx -0.4$ to -0.1 , since model disks often have $(V - I)_{\text{excess}}$ in this range. In conclusion, including the disk component of our spheroidal galaxies has some effect on the predicted distributions, but, with the present dataset, our basic conclusions are insensitive to the presence or absence of a disk component in model galaxies.

So far we have considered most of the parameters of the model to be fixed at the values chosen by Cole et al. (2000), the exceptions being B/Ts and N_{relax} which we have constrained from morphologically selected number counts

and redshift distributions. By adopting this philosophy the model results are true predictions, since the model parameters were fixed by considerations entirely unrelated to star formation activity in spheroidal galaxies.

Finally, we now consider the effect of altering key model parameters which control the formation and merging histories of model galaxies. We will not explore this graphically but it is interesting to examine the consequences qualitatively for two reasons. Firstly, this will aid our understanding of what physical processes are crucial for constraining the statistics we have considered. Secondly, and most importantly, it will test the ability of the type of comparison between theory and observation developed in this paper to place useful constraints on the formation rates of spheroidal galaxies. An important caveat must be borne in mind — namely that after we alter these parameters it is

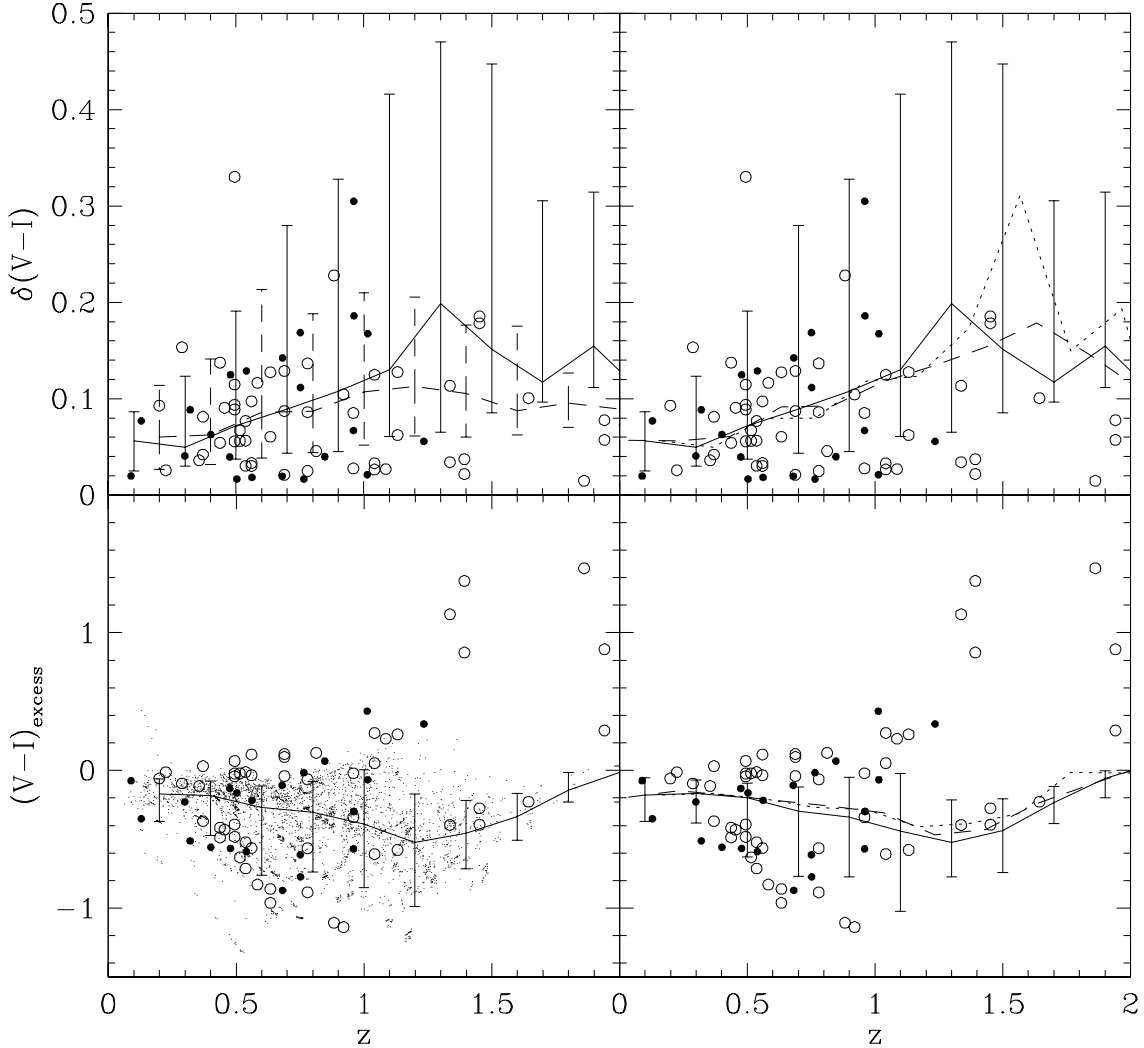


Figure 7. The variation of our two statistics with redshift. Top and bottom rows show $\delta(V - I)$ and $(V - I)_{\text{excess}}$ respectively. In each case circles show HDF galaxies (filled points are spectroscopic redshifts, open points are photometric redshifts). Lines show the median of the model distribution with error bars indicating the 10% and 90% intervals. In the left-hand column the solid line shows results for the Hernquist profile (the dots show a sample of model galaxies to give a more detailed indication of the distribution of model results), while the dashed line shows the result for the $r^{1/4}$ -law profile. In the right-hand column the solid lines show results for our default parameters, while dashed and dotted show results for the alternative B/T_S and alternative N_{relax} respectively.

unlikely that the model will be in as good agreement with the morphologically selected counts and redshift distributions of Figs. 2 & 3 as with the standard set of parameters. Such models are not necessarily physically realistic, and we explore them only to demonstrate the sensitivity of $\delta(V - I)$ and $(V - I)_{\text{excess}}$ to the formation histories of spheroidals.

Three model parameters are crucial to the formation of spheroidals in the model of Cole et al. (2000). The frequency of mergers is controlled by the parameter f_{df} which determines the strength of the dynamical friction force felt by galaxies. The division between minor and major mergers is determined by the parameter f_{ellip} and the timescale of the star burst associated with a major merger depends upon

$\epsilon_{\star, \text{burst}}$. (See §2 and Cole et al. (2000) for further details.) Increasing f_{df} enlarges the merger timescale and so reduces the frequency of the major mergers. Increasing this parameter from 1 to 2 or 4 substantially reduces the number of spheroidal galaxies. The fractional reduction is greatest for high $\delta(V - I)$ (highly negative $(V - I)_{\text{excess}}$) galaxies. This arises since the reduced rate of major mergers means that a given spheroid tends to have experienced its last burst of star formation longer ago, which results in the characteristic colours of the burst stars fading away before the galaxy is observed.

Increasing f_{ellip} to 0.5 or 0.75 also has a large effect on the distributions of $\delta(V - I)$ and $(V - I)_{\text{excess}}$. Firstly, there

is an overall reduction in the number of spheroidals, since major mergers become much rarer. There is also some differential effect, with high $\delta(V-I)$ (equivalently, highly negative $(V-I)_{\text{excess}}$) galaxies being depleted preferentially, again because of the greater time since the most recent merger. A secondary effect of the reduced merger rate is that, particularly at low redshift, galaxies in major mergers tend to be less gas rich when f_{ellip} is increased, as they have had much more time to turn gas into stars quiescently. This also tends to reduce the number of high $\delta(V-I)$ (highly negative $(V-I)_{\text{excess}}$) galaxies.

The parameter $\epsilon_{*,\text{burst}}$ has little effect on the distributions of $\delta(V-I)$ and $(V-I)_{\text{excess}}$ since it does not change the frequency of bursts nor the mass of stars formed within them. It does however alter the sensitivity of the results to the value of N_{relax} . For smaller $\epsilon_{*,\text{burst}}$ we find that increasing N_{relax} produces a greater reduction in the numbers of high $\delta(V-I)$ and highly negative $(V-I)_{\text{excess}}$ galaxies. This occurs because, with the slower star formation rates implied by a low $\epsilon_{*,\text{burst}}$, bursts tend to redden more rapidly and so become indistinguishable from the rest of their galaxy. With $N_{\text{relax}} = 3$ many model spheroidals still have recognisable blue colours to their cores, but for $N_{\text{relax}} = 30$ most have already reddened sufficiently to deplete the highly negative regions of the $(V-I)_{\text{excess}}$ distribution.

The Cole et al. (2000) model assumes that in the case of a minor merger ($M_1/M_2 < f_{\text{ellip}}$) stars from the smaller galaxy are added to the bulge of the larger galaxy, thereby providing a mechanism by which bulges can form without any associated burst of star formation. An alternative would be to assume the stars are added to the disk of the larger galaxy, in which case spheroids can only ever form through a major merger. Cole et al. (2000) found that the choice of where to place stars from minor mergers made little difference to the properties of model galaxies which they considered. We find a similar result, with no significant difference being made to the $\delta(V-I)$ and $(V-I)_{\text{excess}}$ distributions or their redshift dependence.

4 DISCUSSION

We have assessed the implications of the sample of elliptical galaxies in the HDFs with inhomogeneous internal colours (Menanteau, Abraham & Ellis 2001) for the picture of continuous formation of ellipticals expected in hierarchical models of structure formation.

We have shown that the galaxy formation model of Cole et al. (2000) can produce good agreement with data on morphologically selected number counts, and produces many of the trends observed in morphologically selected redshift distributions, although the detailed agreement in these quantities is less good. In defining the morphology of model galaxies we considered the time taken for a merger event to relax to an elliptical galaxy configuration, quantifying this criterion in terms of a multiple, N_{relax} , of the elliptical's dynamical time. Of crucial importance to the present work is that this definition allows a galaxy to be classed as a relaxed elliptical before the distinctive blue colour of recent

star formation has faded. With the present level of agreement between theory and observations it is difficult to set strong constraints on N_{relax} , but $N_{\text{relax}} \lesssim 10$ is favoured, as would be expected on theoretical grounds (Barnes & Hernquist 1992). Accurate determinations of the redshift distribution of elliptical galaxies will provide the strongest constraint on this parameter.

We compare the observational data with model predictions through two statistics, the inhomogeneity index originally defined by Menanteau, Abraham & Ellis (2001) and the difference between the observed $(V-I)$ colour and that of a passively evolving old stellar population at the same redshift (which is simpler to compute from the model, but makes no use of the spatially resolved information in the HDF images and which is sensitive to errors in the photometric redshifts of HDF galaxies).

The theoretical predictions suffer from some uncertainties, due to the rate at which ellipticals are expected to form in a given cosmological model (as demonstrated in Fig. 1), the uncertain spatial distribution of light from recent star formation for which we have only limited theoretical guidance as yet and the parameters used to specify what constitutes a spheroidal galaxy in the model. Nevertheless, we have shown that our basic conclusions are insensitive to the latter two uncertainties (the first is exactly what we are attempting to measure from the data so necessarily has a strong impact on the model predictions), allowing us to make a useful comparison to the observational data.

Comparing our two statistics for model and observed galaxy samples we find reasonable agreement in the distributions of both $\delta(V-I)$ and $(V-I)_{\text{excess}}$ with two notable exceptions. Firstly, the current model produces too few spheroidals with low $\delta(V-I)$ and, secondly, the model does not produce the population of $(V-I)_{\text{excess}} > 0$ galaxies seen in the data. We discuss these two points further below. However, most importantly for the present work is the fact that the model does produce the correct number of high $\delta(V-I)$ and blue $(V-I)_{\text{excess}}$ galaxies. The implication of this result is that a model in which elliptical galaxies form hierarchically in a Λ CDM universe, and which was specifically constrained to match a set of local data (Cole et al. 2000), is quantitatively consistent with the continued star formation implied by the HDF data of Menanteau, Abraham & Ellis (2001) with no further adjustment of the free parameters of the model. The basic trends of $\delta(V-I)$ and $(V-I)_{\text{excess}}$ with redshift are also reproduced by the model. An expanded data set will allow these trends to be tested quantitatively.

However, there is evidence that the model produces somewhat too few relaxed, homogeneous spheroidals from the $\delta(V-I)$ statistic. Given the small sample size and the theoretical uncertainties it is premature to assign much significance to this apparent discrepancy. Perhaps the most noticeable discrepancy between theory and observations is the lack of extremely red objects (relative to a passively evolving spheroidal formed at high redshift) in the model sample. The majority of these objects have only photometric redshifts and so it remains possible that their apparently very red colours for their redshift are simply a consequence of

an incorrect redshift determination. Both of these points should be addressed in more detail, both using larger observational samples, and by improvements in the theoretical calculations.

We have briefly considered the sensitivity of the $\delta(V - I)$ and $(V - I)_{\text{excess}}$ statistics to the formation rate of spheroidals, by varying parameters of the model which directly influence this formation rate. We typically find that lower formation rates tend to preferentially deplete the high $\delta(V - I)$ and highly negative $(V - I)_{\text{excess}}$ regions of the distributions. This is due mainly to the fact that, for a lower spheroidal formation rate, a galaxy's last major merger tends to have occurred longer ago and so the characteristic colours of the recent burst have faded away by the time it is observed. Therefore, analysis of large samples of spheroidals using these techniques should allow us to directly constrain their formation rate.

Spectroscopic observations of these faint populations of ellipticals should allow estimates of their star formation rates and the ages of their stellar populations. These quantities, for which we have presented predictions, can be compared to the theoretical predictions much more directly, and so should provide much stronger constraints on the formation of ellipticals. With the imminent launch of the Advanced Camera for Surveys on Hubble Space Telescope, there is a strong case for assembling a large sample of field spheroidals with redshifts and reliably-sampled internal colours.

ACKNOWLEDGEMENTS

We acknowledge valuable discussions with Bob Abraham, Pieter van Dokkum and Tomasso Treu. AJB thanks his collaborators Carlton Baugh, Shaun Cole, Carlos Frenk and Cedric Lacey for free use of the GALFORM galaxy formation code.

REFERENCES

Abraham R. G., van den Bergh S., Glazebrook K., Ellis R. S., Santiago B. X., Surma P., Griffiths R. E., 1996, ApJS, 107, 1
 Barger A. J., Cowie L. L., Trentham N., Fulton E., Hu E. M., Songaila A., Hall D., 1999, AJ, 117, 102
 Barnes J. E., Hernquist L., 1992, ARA&A, 30, 705
 Barnes J. E., Hernquist L., 1996, ApJ, 471, 115
 Barnes J. E., 1998, in Galaxies: Interactions and Induced Star Formation, Saas-Fee Advanced Course 26. Lecture Notes 1996. Swiss Society for Astrophysics and Astronomy, XIV, Edited by R. C. Kennicutt, Jr., F. Schweizer, J. E. Barnes, D. Friedli, L. Martinet and D. Pfenniger. Springer-Verlag Berlin/Heidelberg, p. 275.
 Baugh C. M., Cole S., Frenk C. S., 1996a, MNRAS, 282, L27
 Baugh C. M., Cole S., Frenk C. S., 1996b, MNRAS, 283, 1361
 Baugh C. M., Cole S., Frenk C. S., Lacey C. G., 1998, ApJ, 498, 504
 Bower R. G., Ellis R. S., Rose J. A., Sharples R. M., 1990, AJ, 99, 530
 Brinchmann J., 1999, Ph.D. thesis, Univ. Cambridge
 Casertano S., de Mello D., Dickinson M., Ferguson H. C., Fruchter A. S., Gonzalez-Lopezlira R. A., Heyer I.,
 Hook R. N., Levay Z., Lucas R. A., Mack J., Makidon R. B., Mutchler M., Smith T., Stiavelli M., Wiggs M. S., Williams R. E., 2000, ApJ, 120, 2747
 Cole S., Lacey C. G., Baugh C. M., Frenk C. S., 2000, MNRAS in press
 Daddi E., Cimatti A., Renzini A., 2000, A&A, 362, 45
 Driver S. P., Windhorst R. A., Ostrander E. J., Keel W. C., Griffiths R. E., Ratnatunga K. U., 1995a, ApJ, 449, L23
 Driver S. P., Windhorst R. A., Griffiths R. E., 1995b, ApJ, 453, 48
 Efstathiou G., Lake G., Negroponte J., 1982, MNRAS, 199, 1069
 Efstathiou G., Silk J., 1983, Fundamentals of Cosmic Physics, 9, 1
 Eggen O. J., Lynden-Bell D., Sandage A. R., 1962, ApJ, 136, 748
 Ellis R. S., Smail I., Dressler A., Couch W. J., Oemler A., Butcher H., Sharples R. M., 1997, ApJ, 483, 582
 Firth A. E. et al., 2001, astro-ph/0108182 (submitted to MNRAS)
 Franceschini A., Silva L., Fasano G., Granato L., Bressan A., Arnouts S., Danese L., 1998, ApJ, 506, 600
 Glazebrook K., Ellis R., Santiago B., Griffiths R., 1995, MNRAS, 275, L19
 Granato G. L., Lacey C. G., Silva L., Bressan A., Baugh C. M., Cole S., Frenk C. S., 2000, ApJ, 542, 710
 Hernquist L., 1992, ApJ, 400, 460
 Im M., Griffiths R. E., Naim A., Ratnatunga K. U., Roche N., Green R. F., Sarajedini V. L., 1999, ApJ, 510, 821
 Im M., Simard L., Faber S. M., Koo D. C., Gebhardt K., Willmer C. N. A., Phillips A., Illingworth G., Vogt N. P., Sarajedini V. L., 2001, astro-ph/0011092
 Kauffmann G., White S. D. M., Guiderdoni B., 1993, MNRAS, 264, 201
 Kauffmann G., 1996, MNRAS, 281, 487
 Kauffmann G., Charlot S., 1998a, MNRAS, 294, 705
 Kauffmann G., Colberg J. M., Diaferio A., White S. D. D., 1999, MNRAS, 303, 188
 Lacey C. G. et al., 2001, in preparation
 Marzke R. O., da Costa L. N., Pellegrini P. S., Willmer C. N. A., Geller M. J., 1998, ApJ, 503, 617
 McCarthy P. J. et al., 2001, astro-ph/0108171 (submitted to ApJ)
 Menanteau F., Ellis R. S., Abraham R. G., Barger A. J., Cowie L. L., 1999, MNRAS, 309, 208
 Menanteau F., Abraham R. G., Ellis R. S., 2001, MNRAS, 322, 1
 Menanteau F., Jimenez R., Matteucci F., 2001, submitted to ApJL
 Mo H. J., Mao S., White S. D. M., 1998, MNRAS, 295, 319
 Sandage A., Visvanathan N., 1978, ApJ, 223, 707
 Sanders D. B., Mirabel I. F., 1996, ARA&A, 34, 749
 Schade D., Lilly S. J., Crampton D., Ellis R. S., Le Fèvre O., Hammer F., Brinchmann J., Abraham R., Colless M., Glazebrook K., Tresse L., Broadhurst T., 1999, ApJ, 525, 31
 Somerville R. S., Primack J. R., Faber S. M., 2001, MNRAS, 320, 504
 Stanford S. A., Eisenhardt P. R., Dickinson M., 1998, ApJ, 492, 461
 Treu T., Stiavelli M., Bertin G., Casertano S., Moller P., 2001, astro-ph/0106147
 van Dokkum P. G., Franx M., Kelson D. D., Illingworth G. D., 1998, ApJ, 504, 17
 van Dokkum P. G., Franx M., Fabricant D., Illingworth G. D., Kelson D. D., 2000, ApJ, 541, 95
 van Dokkum P. G., Franx M., Kelson D. D., Illingworth G. D., 2001, ApJ, 553, 39
 Walker I., Mihos J. C., Hernquist L., 1996, ApJ, 460, 121
 Williams R. E. et al., 1996, AJ, 112, 1335

Zepf S. E., 1997, *Nat.*, 390, 377
Zucca E. et al., 1997, *A&A*, 326, 477